CHINESE JOURNAL OF PHYSICS VOL. 52, NO. 1-I February 2014

Photodetachment of a Hydrogen Negative Ion inside an Annular Nano-Microcavity

De-hua Wang*

School of Physics and Optoelectronic Engineering, Ludong University, Yantai 264025, China

(Received February 26, 2013; Revised April 10, 2013)

The photodetachment of a hydrogen negative ion inside an annular nano-microcavity is studied based on the semiclassical closed orbit theory. The closed orbit of the photo-detached electron in an annular nano-microcavity is investigated and the total photodetachment cross section of this system is calculated. The calculation results suggest that the oscillatory structure in the photodetachment cross section depends on the shape of the microcavity sensitively. If the outer radius R of the annular microcavity is given, with an increase of the inner radius R_{in}, the number of the closed orbits increased correspondingly and the oscillating amplitude in the photodetachment cross section becomes larger. In order to show the correspondence between the cross section and the detached electron's closed orbits clearly, we calculate the Fourier transformation of the cross section and find that each peak corresponds to the length of one closed orbit. We hope that our results will be useful in understanding the photodetachment or the transport and escape process of negative ions in a microcavity.

DOI: 10.6122/CJP.52.138 PACS numbers: 05.45.Ac, 34.35.+a, 32.80.Gc, 31.15.xg

I. INTRODUCTION

The study of the correspondence between classical and quantum mechanics is an interesting topic in atomic physics. Since the development of closed orbit theory (COT) for studying the photoabsorption spectra of the hydrogen atom in a strong magnetic field [1], it has become an important tool to study the connections between the classical mechanics of the macroscopic world and the quantum mechanics of the microscopic world. Firstly, COT was used to study the photoabsorption spectra of the Rydberg atoms or molecules in strong external electric and magnetic fields [1–5]; then it was developed to study the photodetachment of a negative ion in external fields [6–10]. Closed orbit theory relates the oscillating structure in the photodetachment cross section of a negative ion in external electric and magnetic fields to the closed orbits of the detached electron. Recently, with the development of surface physics and photodetachment microscopy, closed orbit theory has been used to study the photodetachment of a negative ion near surfaces [11–25]. First, Yang, Du, and Wang *et al.* studied the photodetachment of H^- near an elastic interface based on the closed orbit theory [11–14]. Later, they studied the photodetachment of H^- near

*Electronic address: lduwdh@163.com

metal surfaces [15–25]. Very recently, Zhao and Du studied the photodetachment of H^- in an open wedge cavity [26]. In these previous studies, they all studied the photodetachment of a negative ion near surfaces or inside an open cavity. As to the photodetachemnt of a negative ion inside a closed microcavity, the studies have been relatively few. In our recent work, we studied the photodetachment of H^- inside a closed square or circular microcavity [27]. But a square or circular microcavity is the simplest model. There is no interesting parameter to vary, since the length of the detached-electron's orbit is only related to the length of the square side or the radius of the circular microcavity. In order to further probe the correspondence between the classical mechanics and the quantum mechanics of some complex systems, we extend the analyses of these simple systems to more complex cases. In this work, we study the photodetachment of H^- inside an annular nano-microcavity. In our study, we still neglect the interaction between the detached electron and the surfaces and consider the surfaces of the annular microcavity as elastic ones [11–13]. The electron follows a straight line trajectory inside the microcavity until it is reflected by the surfaces of the microcavity. Therefore, the electron bounces between the surfaces like a particle in an annular billiard [28–30]. In comparison with the circular microcavity [31], the classical closed orbits for the annular microcavity have a far richer structure than the corresponding purely circular case, and the pattern of the allowed classical closed orbits varies dramatically as the relative size of the inner annulus is increased [29]. Our study shows that an oscillating structure appears in the photodetachment cross section, which is a consequence of the interference effects of the returning electron waves with the outgoing waves traveling along the closed orbits. Besides, our study suggests that the photodetachment cross section of the negative ion depends on the laser polarization and the shape of the nano-microcavity sensitively. If the outer radius of the annular billiard is given, as we vary the value of the inner radius, the oscillating structure in the cross section changes accordingly.

This paper is organized as follows: In Section II, we first give a physical picture description for the classical motion of the photo-detached electron inside an annular nano-microcavity, then we give the formula for calculating the photodetachment cross section. In Section III, we calculate the photodetachment cross section of a negative ion inside an annular microcavity with different inner annulus. Then we compare the difference in the Fourier transformed cross section between different annular microcavities. Finally, some conclusions of this paper are given in Section IV. Atomic units are used throughout this work unless indicated otherwise.

II. THEORY AND QUANTITATIVE FORMULA

II-1. Physical picture description

In Fig. 1, we show the schematic plot of the system. The H^- ion is assumed to be at the origin. A linearly polarized laser is used for the photodetachment. The annular microcavity is placed in the x-y plane, with x-axis along one diameter. Suppose the outer radius of the nano-microcavity is R and the inner radius is $R_{in} = fR$, $0 < f < 1$. As in the previous studies, H^- can be considered as a one-electron system, with the active electron

loosely bound by a short-ranged, spherically symmetric potential of the hydrogen atom [6–10]. According to the physical picture of closed orbit theory (COT) [1, 10], when the active electron is photo-detached by a laser, it is detached and the associated wave propagates out from the negative ion in all directions. The electron trajectories follow a straight line inside the microcavity until they are bounced back by the inner or outer surfaces of the microcavity. After one or several bounces of the surfaces, the electron may return to the origin of the negative ion, in which case the returning electron waves will interfere with the outgoing source waves to produce an oscillatory structure in the photodetachment cross section. COT relates the oscillations in the photodetachment cross sections with all the closed orbits of the detached electron. Therefore, in order to calculate the photodetachment cross section, we must find out all the closed orbits of the photodetached electron. In Fig. 1, we plot a group of the detached-electron's trajectories near a closed orbit.

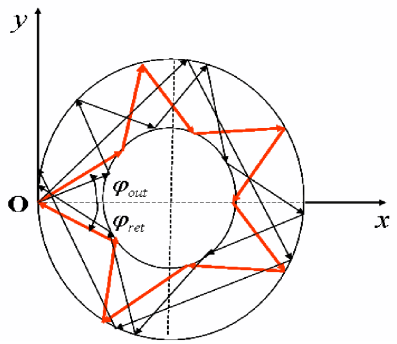

FIG. 1: Schematic illustration of H^- photodetachment inside an annular nano-microcavity. The H^- lies at the origin and the mircorcavity is in the $x-y$ plane. A group of trajectories propagate away from the H atom and finally return to the region of the atom after being reflected several times by the inner and outer surfaces of the microcavity. The closed orbit is marked by the red line.

II-2. Closed orbits search

We now search for all the closed orbits of the electron in an annular nano-microcavity. The potential in the annular microcavity can be defined as follows [28]:

$$V(r) = \begin{cases} 0 & \text{for } R_{in} < r < R_{out}, \\ \infty & \text{otherwise.} \end{cases} \tag{1}$$

Since the electron's motion in the annular microcavity is the same as that of an annular billiard [28, 29], we can use the same method for finding the periodic orbits in the annular billiard to find the closed orbits of the detached electron. There are three kinds of closed orbits.

First, the electron leaves the atom along the diameter direction with the outgoing angle $\varphi_{out} = 0$, after being reflected by the inner surface of the annulus, it then retraces back to the atom. This orbit is called the "back-and-forth orbit". The length of this kind

of closed orbit is

$$L^{(1)} = n[2(1-f)]R, \tag{2}$$

where n represents the repetition number of the primitive back-and-forth orbit.

The second kind of closed orbit is the same as the ones in the circular billiard [28, 29, 31], which can be denoted by a pair of integers (p, q) to distinguish different closed orbits. Where p and q are non-negative integers, $p > 2q$. p denotes the number of the bounces on the surface of the microcavity and q counts the number of rotations made by the particle before returning to the origin in phase space. If p and q share a common factor n, $p = n\tilde{p}$, $q = n\tilde{q}$, then orbits labeled by $(p, q) = n(\tilde{p}, \tilde{q})$ can be considered as an n-fold repetition of the primitive orbit $(\tilde{p}, \tilde{q})$ [31]. For $q > 2$, the shapes of the closed orbit are polygons. The outgoing angle of the electron relative to the x-axis is: $\varphi_{out} = \frac{\pi}{2} - \frac{q\pi}{p}$. The corresponding returning angels of each closed orbit are given by: $\varphi_{ret} = \pi - \varphi_{out}$. For the annular microcavity, these closed orbits still exist, provided that the closest distance from the center of the annular to the polygon $R_{\min} = R\cos(\frac{q\pi}{p})$ is larger than the radius of the inner radius R_{in} [28, 29]. This condition can be reduced to $p \geq \pi q/\arccos(f)$. This kind of closed orbit can be described as follows: The electron is emitted from the origin and moves away in all directions. After one or several reflections of the outer surface of the annular microcavity, the electron returns to the origin to form a closed orbit. This kind of closed orbit does not bounce off the inner annulus and is still characterized by a pair of integers (p, q). The length of this kind of the closed orbit is

$$L^{(2)} = 2pR\sin\left(\frac{\pi q}{p}\right). \tag{3}$$

In Fig. 2, we plot some of this kind of closed orbits.

The third kind of closed orbit is still characterized by the same pair of integers (p, q), but they bounce off the inner annulus. This kind of closed orbit are still only supported provided that $p \geq \pi q/\arccos(f)$. The length of these closed orbits is given by [28, 29]

$$L^{(3)} = 2pR\sqrt{1 + f^2 - 2f\cos\left(\frac{\pi q}{p}\right)}. \tag{4}$$

The outgoing angle of the electron relative to the x-axis is

$$\varphi_{out} = \arccos\left[\frac{1 - f\cos(\pi q/p)}{\sqrt{1 - 2f\cos(\pi q/p) + f^2}}\right]. \tag{5}$$

The corresponding returning angles of each closed orbit are given by $\varphi_{ret} = \pi - \varphi_{out}$.

In Fig. 3, we plot some of this kind of closed orbits. The ratio of the inner and outer radius of the annular microcavity is $f = 0.5$. Under this condition, only those orbits with $p \geq 3q$ can exist. Fig. 3(a) shows the (3,1) closed orbit, which is an equilateral triangle. For $p = 3$, $q = 1$, $f = 0.5$, the closest distance from the center of the annular to the triangle

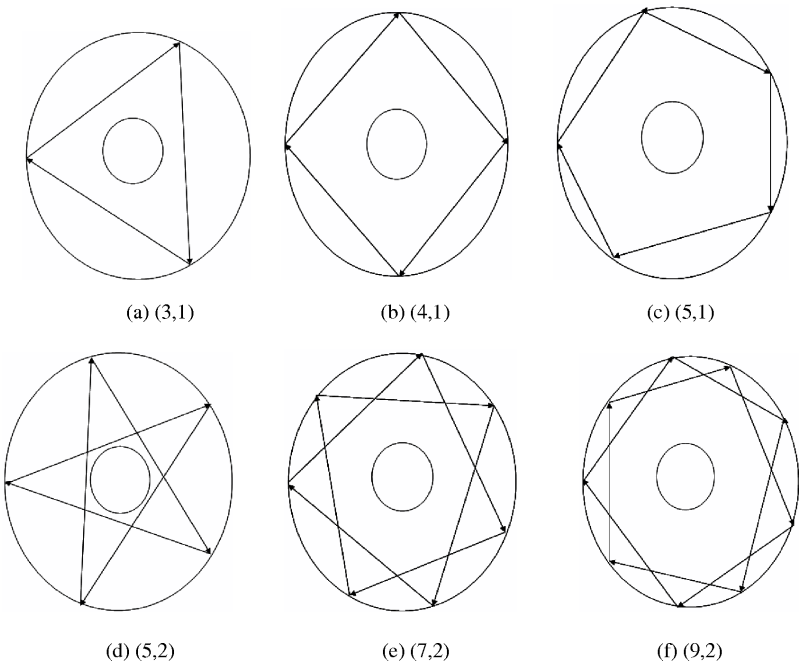

FIG. 2: Some typical closed orbits of the second kind of the detached electron inside an annular nano-microcavity. The numbers of p and q are given in each plot.

is $R_{\min} = R\cos(\frac{q\pi}{p}) = 0.5R = R_{in}$. Thus this triangle is tangent to the inner surface of the annular microcavity. This orbit leaves the atom with the outgoing angle $\varphi_{out} = 30^0$, after skimming over the inner annulus, it then bounced off the outer surface of the annulus. After being reflected by the outer surface twice, it then returns back to the atom. Fig. 3(b) shows the (4,1) closed orbit. This orbit leaves the atom with the outgoing angle $\varphi_{out} = 28.67^0$, after bouncing off the inner and outer surfaces of the annular microcavity four times, it returns back to the atom. Similar descriptions can be given for other closed orbits.

In our calculation, we suppose the outer radius of the annular nano-microcavity $R =$ 100 a.u. $\approx$ 5.3 nm. In Tables I–III, we summarize the collision number p, rotation number q, and the length L of the three kinds of closed orbit with the length $L \leq 1400$ a.u. ≈ 74.2 nm. for different inner radii of the annular microcavity. In our calculation, we include only those closed orbits with $2 \leq p \leq 10$ and $1 \leq q \leq 3$. Due to the symmetry of the annular microcavity, we only give out the closed orbit with the outgoing angle $0 \leq \varphi_{out} \leq 90°$. The length, collision and rotation number of those closed orbits with $-90° < \varphi_{out} \leq 0°$ are the same as the ones with $-\varphi_{out}$.

II-3. Photodetachment cross section

For the annular microcavity, the same procedure as given in the derivation of the photodetachment cross section of H^- in a square or circular microcavity can be used [27]. For simplicity, we only briefly summarize the results. According to the closed orbit theory,

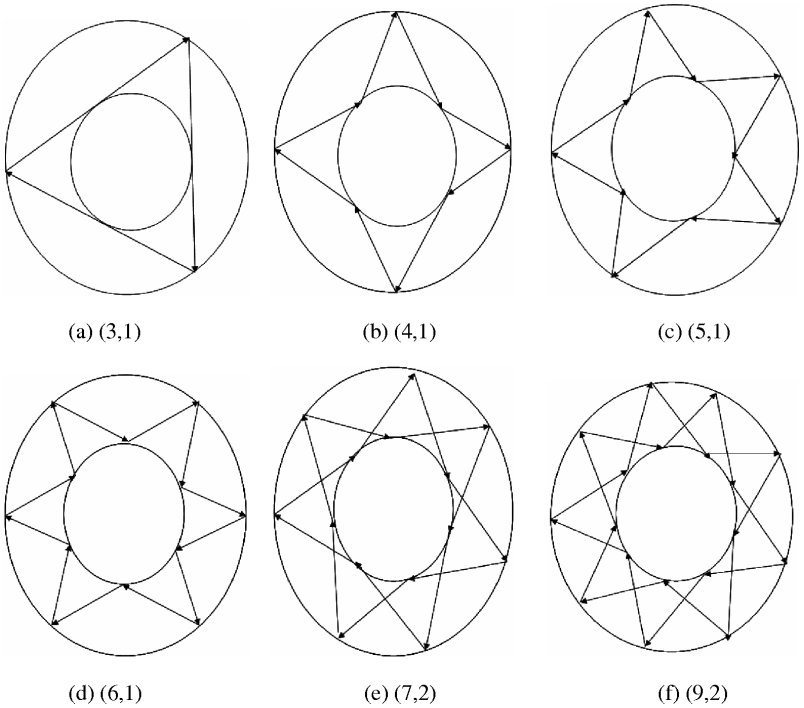

FIG. 3: Some typical third kind closed orbits of the detached electron inside an annular nano-microcavity. The numbers of p and q are given in each plot.

the photodetachment cross section of H^- in a microcavity can be written as

$$\sigma(E) = \sigma_0(E) + \sigma_{osc}(E), \tag{6}$$

in which $\sigma_0(E) = \frac{16\sqrt{2}\pi^2 B^2 E^{3/2}}{3c(E_b+E)^3}$ is the smooth background term of H^- in free space without microcavity [11]. $\sigma_{osc}(E)$ is the oscillating term, which is given by [27]

$$\sigma_{osc}(E) = \frac{16\pi^2 B^2 E}{c(E_b+E)^3} \sum_j \frac{1}{L_j} \chi(\theta^j_{out}, \varphi^j_{out}) \chi^*(\theta^j_{ret}, \varphi^j_{ret}) \sin(kL_j - \mu_j \pi/2), \tag{7}$$

where the summation includes all the detached electron's closed orbits. L_j is the length of the closed orbits, and μ_j is the Maslov index. $\theta^j_{out}, \varphi^j_{out}$ are the polar and outgoing angles, while $\theta^j_{ret}, \varphi^j_{ret}$ are the polar and returning angles of the jth closed orbit. Since all the closed orbits lie in the x-y plane, then the polar angles of the closed orbit $\theta^j_{out} = \theta^j_{ret} = \pi/2$. $\chi(\theta^j_{out}, \varphi^j_{out}) \chi^*(\theta^j_{ret}, \varphi^j_{ret})$ is an angular factor, which is related to the laser polarization. For the x and y polarization laser light, the angular factor can be written as [27]

$$\begin{aligned} \chi_x(\theta^j_{out}, \varphi^j_{out}) \chi^*_x(\theta^j_{ret}, \theta^j_{ret}) &= \cos\varphi^j_{out} \cos\varphi^j_{ret}, \\ \chi_y(\theta^j_{out}, \varphi^j_{out}) \chi^*_y(\theta^j_{ret}, \theta^j_{ret}) &= \sin\varphi^j_{out} \sin\varphi^j_{ret}. \end{aligned} \tag{8}$$

TABLE I: The geometry parameters of the three kinds of the closed orbit inside the annular microcavity, the inner radius $R_{in} = 0.1R$, $R = 100$ a.u.

first kind		second kind		third kind	
n	$L^{(1)}$ (a.u.)	(p,q)	$L^{(2)}$ (a.u.)	(p,q)	$L^{(3)}$ (a.u.)
1	180	(3,1)	519.62	(3,1)	572.36
2	380	(4,1)	565.68	(4,1)	745.58
3	540	(5,1)	587.78	(5,1)	920.97
4	720	(6,1)	600.00	(6,1)	1097.71
5	900	(7,1)	607.43	(7,1)	1275.31
6	1080	(8,1)	612.29	(5,2)	973.75
7	1260	(9,1)	615.63	(6,2)	1144.72
		(10,1)	618.03	(7,2)	1317.26
		(5,2)	951.05	(7,3)	1375.63
		(6,2)	1039.23		
		(7,2)	1094.56		
		(8,2)	1131.37		
		(9,2)	1157.01		
		(10,2)	1175.57		
		(7,3)	1364.90		

Therefore, the total photodetachment cross section of H^- in an annular microcavity for x-polarized light is given by [27]

$$\sigma_x(E) = \sigma_0(E) + \frac{16\pi^2 B^2 E}{c(E_b+E)^3} \sum_j \frac{1}{L_j} \cos\varphi^j_{out} \cos\varphi^j_{ret} \sin(kL_j - \mu_j\pi/2). \tag{9}$$

For y-polarized light,

$$\sigma_y(E) = \sigma_0(E) + \frac{16\pi^2 B^2 E}{c(E_b+E)^3} \sum_j \frac{1}{L_j} \sin\varphi^j_{out} \sin\varphi^j_{ret} \sin(kL_j - \mu_j\pi/2). \tag{10}$$

II-4. Fourier transformed photodetachment cross section

In order to show the correspondence between the oscillating cross section and the detached electron's closed orbits, we perform the Fourier transformation (FT) of the photodetachment cross section. The Fourier transformation of the cross section is defined as

$$F(L') = \int_{k_1}^{k_2} [\sigma(E) - \sigma_0(E)] \exp(-ikL')dk. \tag{11}$$

TABLE II: The geometry parameters of the three kinds of the closed orbit inside the annular microcavity, the inner radius $R_{in} = 0.3R$, $R = 100$ a.u.

	first kind	second kind		third kind	
n	$L^{(1)}$ (a.u.)	(p,q)	$L^{(2)}$ (a.u.)	(p,q)	$L^{(3)}$ (a.u.)
1	140	(3,1)	519.62	(3,1)	533.29
2	280	(4,1)	565.68	(4,1)	652.74
3	420	(5,1)	587.78	(5,1)	777.55
4	560	(6,1)	600.00	(6,1)	906.28
5	700	(7,1)	607.43	(7,1)	1037.71
6	840	(8,1)	612.29	(8,1)	1171.03
7	980	(9,1)	615.63	(9,1)	1305.69
8	1120	(10,1)	618.03	(5,2)	951.10
9	1260	(5,2)	951.05	(6,2)	1066.58
10	1400	(6,2)	1039.23	(7,2)	1184.55
		(7,2)	1094.56	(8,2)	1305.48
		(8,2)	1131.37		
		(9,2)	1157.01		
		(10,2)	1175.57		

In which L' is the geometric length of the closed orbit. Therefore, the Fourier transformation of the photodetachment cross section will show features at values of L' corresponding to the length of classical closed orbits. For finite length of the closed orbit, $F(L')$ is a complex number. In our calculations, we calculate $|F(L')|^2$.

III. RESULTS AND DISCUSSIONS

Using Eqs. (9)–(10) and the above formula for the length L, the outgoing angle φ_{out} and returning angel φ_{ret} of the closed orbit, we calculate the photodetachment cross section of H^- in an annular nano-microcavity. In the following calculation, we fix the outer radius of the annular microcavity at $R = 100$ a.u. ≈ 5.3 nm.

Firstly, we choose a specific annular microcavity with the inner radius $R_{in} = 0.3R$ ≈ 1.6 nm. The calculation results are given in Figs. 4–5. Fig. 4 shows the total photodetachment cross sections for the laser light polarized along the x-direction. Fig. 4(a) is the cross section with the length of the closed orbit $L \leq 500$ a.u. The oscillatory structure appears in the cross section in contrast to the smooth curve without the microcavity, but

TABLE III: The geometry parameters of the three kinds of the closed orbit inside the annular microcavity, the inner radius $R_{in} = 0.5R$, $R = 100$ a.u.

	first kind	second kind		third kind	
n	$L^{(1)}$ (a.u.)	(p,q)	$L^{(2)}$ (a.u.)	(p,q)	$L^{(3)}$ (a.u.)
1	100	(3,1)	519.62	(3,1)	519.62
2	200	(4,1)	565.68	(4,1)	589.45
3	300	(5,1)	587.78	(5,1)	664.06
4	400	(6,1)	600.00	(6,1)	743.58
5	500	(7,1)	607.43	(7,1)	827.10
6	600	(8,1)	612.29	(8,1)	913.71
7	700	(9,1)	615.63	(9,1)	1002.69
8	800	(10,1)	618.03	(10,1)	1093.51
9	900	(6,2)	1039.23	(6,2)	1039.23
10	1000	(7,2)	1094.56	(7,2)	1108.13
11	1100	(8,2)	1131.37	(8,2)	1178.90
12	1200	(9,2)	1157.01	(9,2)	1252.20
13	1300	(10,2)	1175.57	(10,2)	1328.13
14	1400				

the oscillating amplitude and frequency is relatively small. The reason can be analyzed as follows: As $f = 0.3$, only the orbits with $p \geq 2.48q$ in the second and third kind of closed orbit can exist except for the back-and-forth closed orbit. If we choose $q = 1$, then $p = 3$, the smallest length of the second and third kind closed orbit is 519.61 and 533.29 a.u. Therefore, they have no contribution to the photodetachment cross section. Under this condition, only the back-and-forth closed orbit and their repetitions contribute to the cross section. Thus the oscillating amplitude and frequency in the cross section is relatively small. With an increase of the length of the closed orbit, the number of the closed orbit increases correspondingly, and the amplitude and the frequency of the cross section are apparently increased, as we can see from Fig. 4(b–d). The reasons can be explained using the closed orbit theory: the oscillation in the photodetachment cross section is caused by the interference effect between the outgoing waves and the returning waves traveling along the closed orbits. The more the closed orbits, the more the returning waves bounced back by the surfaces of the microcavity; therefore, their contribution to the cross section becomes significant [10].

Fig. 5 shows the total photodetachment cross sections for the laser light polarized along the y-direction. The lengths of the closed orbit are the same as the ones given in

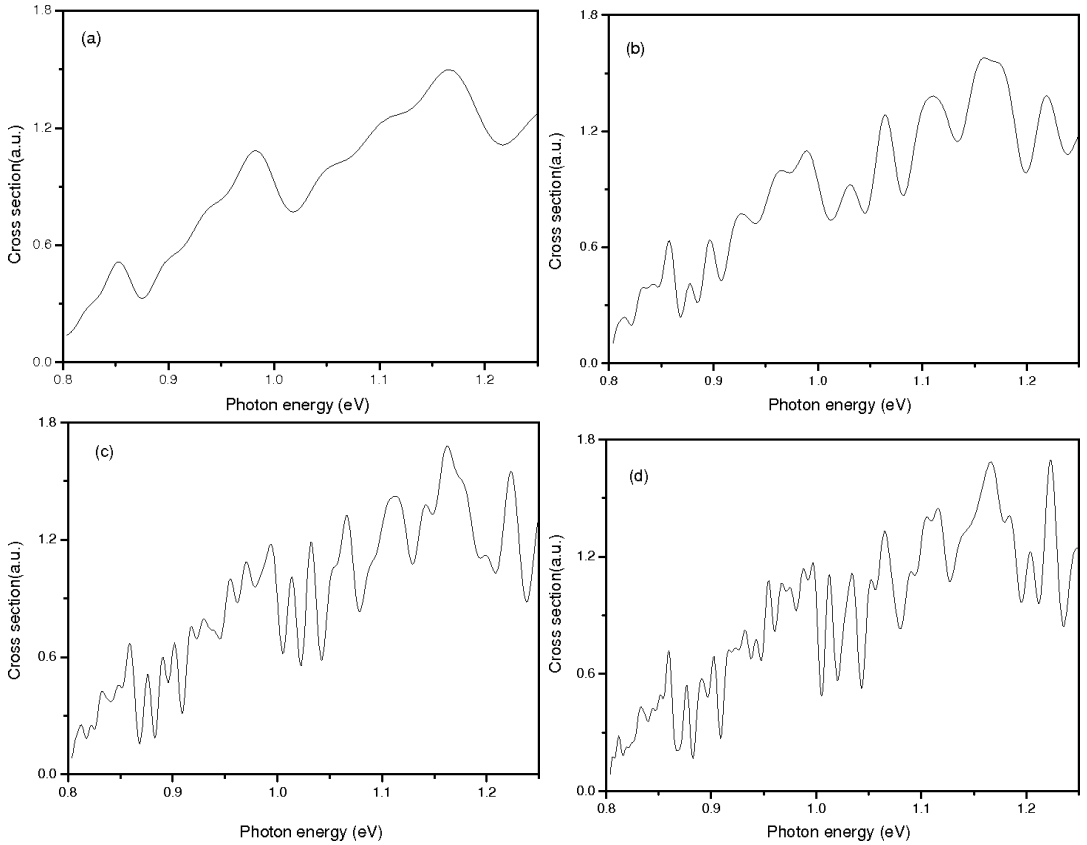

FIG. 4: The photodetachment cross section of H^- in an annular nano-microcavity with different lengths of the closed orbit. The inner radius of the annular microcavity is $R_{in} = 0.3R$ and the laser is linearly polarized in the x-direction. (a) $L \leq 500$ a.u., (b) $L \leq 1000$ a.u., (c) $L \leq 1500$ a.u., (d) $L \leq 2000$ a.u.

Fig. 4. By comparing Fig. 5 with Fig. 4, we find with the increase of the length of the closed orbit, the oscillation in the cross section becomes complex for both cases, but the oscillatory structures are different. For example, in Fig. 5(a), there is no obvious oscillatory structure in the cross section, and the cross section is the same as the one without the microcavity. The reason is as follows: As the length of the closed orbit $L \leq 500$ a.u., only the back-and-forth closed orbits with the outgoing angles $\varphi_{\text{out}} = 0$ contribute to the cross section. From Eq. (10), we find that as the angle $\varphi_{\text{out}} = 0$, the factor sin in the oscillating cross section is also 0, therefore, their contribution to the cross section disappears. Besides, the oscillating amplitude for the laser light polarized along the y-direction is smaller than the case of the laser light polarized along the x-direction. For y-polarized laser light, the oscillating structure is dominated by high-frequency oscillations, whereas for x-polarized laser light, the oscillating structure is dominated by low-frequency oscillations. From the above two figures, we conclude that the photodetachment cross section of H^- in an annular microcavity depends both on the length of the closed orbits and the laser polarization.

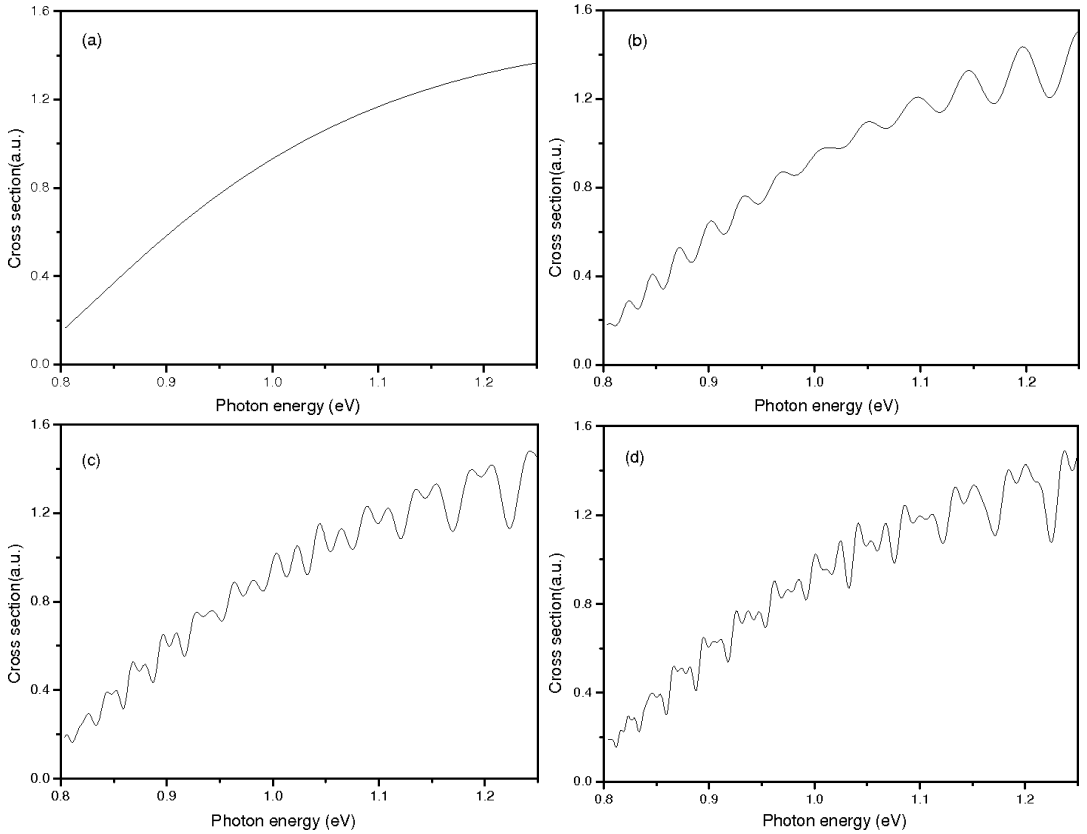

FIG. 5: The photodetachment cross section of H^- in an annular nano-microcavity with different lengths of the closed orbit. The inner radius of the annular microcavity is $R_{in} = 0.3R$ and the laser is linearly polarized in the y-direction. (a) $L \leq 500$ a.u., (b) $L \leq 1000$ a.u., (c) $L \leq 1500$ a.u., (d) $L \leq 2000$ a.u.

Next, we calculate the photodetachment cross section of H^- in an annular microcavity with the length of the closed orbit $L \leq 1400$ a.u. ≈ 74.2 nm. for different values of the inner radius. In our calculation, we do not include all of the possible orbit length formulas in order for the plot to remain distinguishable. We include only those closed orbits with $2 \leq p \leq 10$ and $1 \leq q \leq 3$, and we only consider the case with the laser light polarized along x-direction. The results are given in Fig. 6. Fig. 6(a) is the case of the inner radius $R_{in} = 0.0$, which is the cross section of the circular microcavity. Figs. 6(b–d) are the cross sections of the annular microcavity with the inner radius $R_{in} = 0.1R$, $0.3R$, and $0.5R$, respectively. From this figure, we find the oscillating structure of the cross section in the annular microcavity is more complex than in the circular microcavity. Besides, with the increase of the inner radius of the annular microcavity, the oscillating structure in the cross section becomes much more complex and the oscillating amplitude becomes larger. The reason can be analyzed as follows: from Table I–III, we can see with the increase of the inner radius of the annular nano-microcavity, the number of the closed orbit increased

correspondingly. For example, when $R_{in} = 0.1R$, there is altogether 31 closed orbits; when $R_{in} = 0.3R$, the number of the closed orbits is increased to 35; as $R_{in} = 0.5R$, the number of the closed orbit is further increased to 40. With an increase of the number of closed orbits, the returning waves bounced back by the inner and outer surfaces of the microcavity become more, which leads to a large oscillation and amplitude in the photodetachment cross section. If we further increase the inner radius of the annular microcavity, the number of the closed orbit will become larger and the oscillatory structure in the photodetachment cross section will become much more complex.

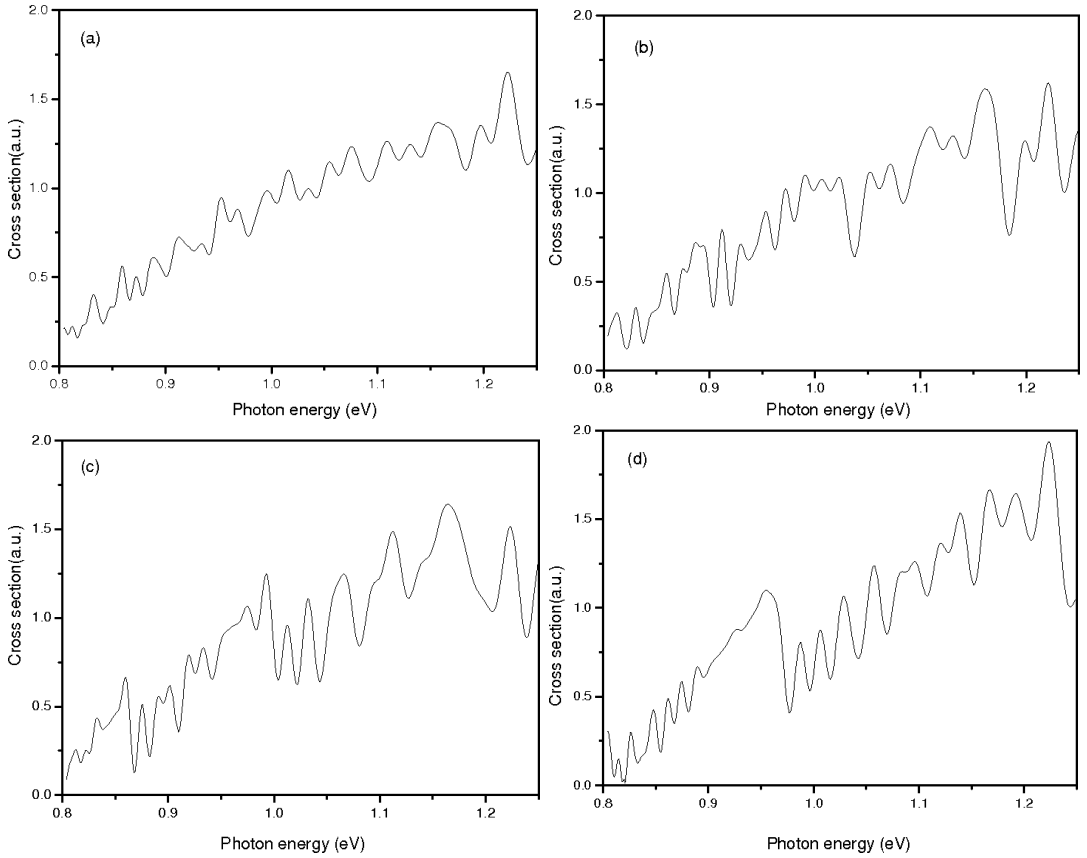

FIG. 6: The photodetachment cross section of H^- in an annular nano-microcavity with different inner radii. The length of the closed orbit $L \leq 1400$ a.u., and the laser is linearly polarized in the x-direction. (a) $R_{in} = 0.0$, which is the case of the circular microcavity, (b) $R_{in} = 0.1R$, (c) $R_{in} = 0.3R$, (d) $R_{in} = 0.5R$.

Finally, in order to show the correspondence between the cross section and the detached electron's closed orbits clearly, we calculated the Fourier transformation of the cross section with laser polarization along the x-axis. The calculation was carried out using $k_1 = 0.027a_0^{-1}$, $k_2 = 0.86a_0^{-1}$, and a step size $\Delta k = 0.001a_0^{-1}$. The result is given in Fig. 7. In our calculation, we still include only those closed orbits with $2 \leq p \leq 10$ and $1 \leq q \leq 3$.

Fig. 7(a) is the Fourier transformed cross section with the negative ion lies in the circular microcavity. Figs. 7(b–c) show the cross sections of H^- lying in the annular microcavity with the inner radius $R_{in} = 0.1R$, $0.3R$, and $0.5R$, respectively. This figure suggests that the number of the peaks is increased with an increase of the inner radius; all the lengths of the closed orbits can be found from Table I–III. Besides, by comparing Fig. 7(a) with Figs. 7(b–c), we find that the number of the peaks in the annular microcavity is more than that in the circular microcavity. In our calculation, we only consider the annular microcavity with the maximum inner radius $R_{in} = 0.5R$. If the inner radius $R_{in} > 0.5R$, the number of the closed orbit will become larger and the peaks in the Fourier transformed photodetachment cross section will become much more complex, which will make the plot unreadable.

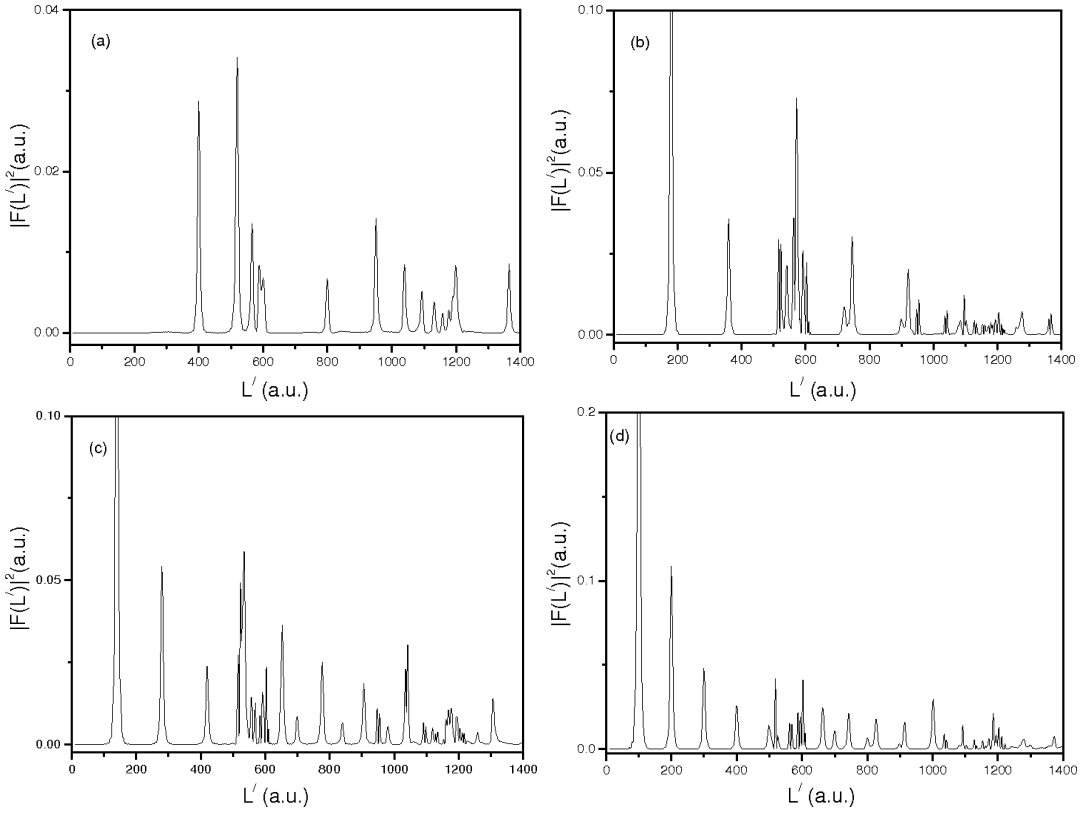

FIG. 7: The Fourier transformed photodetachment cross section of H^- in an annular nano-microcavity with different inner radii. (a) $R_{in} = 0.0$, which is the case of the circular microcavity, (b) $R_{in} = 0.1R$, (c) $R_{in} = 0.3R$, (d) $R_{in} = 0.5R$.

IV. CONCLUSIONS

In summary, we have investigated the photodetachment of H^- in an annular nano-microcavity by using the closed orbit theory. The photodetachment of H^- in the annular microcavity exhibits three main features. First, the number of the detached electron's closed orbit is larger than in the circular microcavity; second, the amplitude and frequency of photodetachment cross sections have a strong dependence on the inner radius of the microcavity. With an increase of the inner radius, the number of the closed orbit increases and the oscillating amplitude in the photodetachment cross section becomes larger. Third, the total photodetachment cross section is related to the laser polarization sensitively. In this work, we have made the calculation by assuming that the negative ion lies inside the annular microcavity. It is relatively easy to imagine more complex systems for which the application of such a more specialized analysis would prove profitable. For example, the spherical microcavity can be considered as a generalization of the circular microcavity and similar calculations can be carried out. At present, studies of the ion-surface interaction are becoming increasingly important in the development of negative-ion photodetachment microscopy experiments, surface chemistry and analysis, reactive ion etching, escape and transport, etc. We hope that our studies will be useful in guiding the future theoretical and experimental research of the photodetachment or the escape and transport process of negative ions near a surface or inside a microcavity.

Acknowledgements

This work was supported by the National Natural Science Foundation of China under Grant Nos. 11374133,11074104 & 10604045, and a Project of Shandong Province Higher Educational Science and Technology Program of China under Grant No. J13LJ04.

References

[1] M. L. Du and J. B. Delos, Phys. Rev. A **38**, 1896 (1988).
[2] J. Gao and J. B. Delos, Phys. Rev. A **46**, 1449 (1992).
[3] B. Hüpper, J. Main, and G. Wunner, Phys. Rev. Lett. **74**, 2650 (1995).
[4] A. Matzkin, P. A. Dando, and T. S. Monteiro, Phys. Rev. A **66**, 013410 (2002).
[5] D. H. Wang and S. L. Ding, Phys. Rev. A **68**, 023405 (2003); Phys. Rev. A **71**, 013420 (2005).
[6] M. L. Du and J. B. Delos, Phys. Rev. A **38**, 5609 (1988).
[7] A. D. Peters and J. B. Delos, Phys. Rev. A **47**, 3020 (1993).
[8] Z. Y. Liu and D. H. Wang, Phys. Rev. A **54**, 4078 (1996); **55**, 4605 (1997).
[9] A. D. Peter, C. Jaffe, J. Gao, and J. B. Delos, Phys. Rev. A. **56**, 345 (1997).
[10] M. L. Du, Phys. Rev. A **70**, 055402 (2004).
[11] G. C. Yang, Y. Z. Zheng, and X. X. Chi, J. Phys. B **39**, 1855 (2006).
[12] G. C. Yang, Y. Z. Zheng, and X. X. Chi, Phys. Rev. A **73**, 043413 (2006).
[13] D. H. Wang, Eur. Phys. J. D **45**, 179 (2007).
[14] A. Afaq and M. L. Du, J. Phys. B **40**, 1309 (2007).

[15] H. J. Zhao and M. L. Du, Phys. Rev. A **79**, 023408 (2009).
[16] K. K. Rui and G. C. Yang, Surf. Sci. **603**, 632 (2009).
[17] B. C. Yang and M. L. Du, J. Phys. B **43**, 035002 (2010).
[18] T. T. Tang and D. H. Wang, J. Phys. Chem. C **115**, 20529 (2011).
[19] Y. Han, L. F. Wang, S. Y. Ran, and G. C. Yang, Phys. B **405**, 3082 (2010).
[20] K. Y. Huang and D. H. Wang, J. Phys. Chem. C **114**, 8958 (2010).
[21] D. H. Wang, J. Appl. Phys. **109**, 014113 (2011).
[22] D. H. Wang, S. S. Wang, and T. T. Tang, J. Phys. Soc. Jpn. **80**, 094301 (2011).
[23] M. Haneef, I. Ahmad, A. Afaq, and A. Rahman, J. Phys. B **44**, 195004 (2011).
[24] D. H. Wang, S. S. Li, and H. F. Mu, J. Phys. Soc. Jpn. **81**, 074301 (2012).
[25] D. H. Wang, Curr. Appl. Phys. **11**, 1228 (2011).
[26] H. J. Zhao and M. L. Du, Phys. Rev. E **84**, 016217 (2011).
[27] D. H. Wang and S. S. Li, J. Phys. Soc. Jpn. **81**, 114301 (2012); D. H. Wang and S. S. Li, Chin. Phys. B **22**, 073401 (2013).
[28] R. W. Robinett, Surf. Rev. Lett. **5**, 519 (1998).
[29] R. W. Robinett, Am. J. Phys. **67**, 67 (1999).
[30] M. Hentschel and K. Richter, Phy. Rev. E **66**, 056207 (2002).
[31] R. W. Robinett, J. Math. Phys. **39**, 278 (1998).